Holzforschung, Vol. 64, pp. 699–704, 2010 • Copyright © by Walter de Gruyter • Berlin • New York. DOI 10.1515/HF.2010.104

Characteristics and discrimination of five types of wood-plastic composites by FTIR spectroscopy combined with principal component analysis

Chia-Huang Lee, Tung-Lin Wu, Yong-Long Chen and Jyh-Horng Wu*

Department of Forestry, National Chung Hsing University, Taichung, Taiwan

*Corresponding author.
Department of Forestry, National Chung Hsing University, Taichung 402, Taiwan
Phone: +886-4-22840345
Fax: +886-4-22851308
E-mail: eric@nchu.edu.tw

Abstract

The analytical potential of attenuated total reflection-Fourier transform infrared (ATR-FTIR) spectroscopy has been tested on the following wood-plastic composites (WPCs): high and low density polyethylene (HDPE and LDPE), polypropylene (PP), polystyrene (PS), and a recycled plastic (rHDPE). The data set of ATR-FTIR spectra has been analyzed by principal component analysis (PCA) and the studied samples could be grouped according to their polymeric matrixes. Additionally, ATR-FTIR spectroscopy proved to be a useful tool for determining the distribution profile of wood and plastic materials within different types of WPCs. Accordingly, the plastic content of the surface layers of HDPE, rHDPE, and PP composites was significantly higher than that of the core layer, whereas homogenous dispersion was observed in the LDPE composite. Among all WPCs, the PS composite displayed the worst dispersion.

Keywords: attenuated total reflection-Fourier transform infrared (ATR-FTIR); distribution profile; principal component analysis; recycled plastic; wood-plastic composites.

Introduction

Wood-plastic composites (WPCs) belong to one of the most dynamic sectors in the plastics industry (Rothlin 2007). The global WPC market has been experiencing double digit growth in North America and Europe (Ashori 2008; Lei and Wu 2010), and a share of WPC decking in the market is forecasted to grow more than 30% in 2011 (Klyosov 2007). Virgin thermoplastics, such as high and low density polyethylene (HDPE and LDPE), polypropylene (PP), and polystyrene (PS), are the best known WPC products (Nair et al. 2001; Harper and Wolcott 2004; Bengtsson et al. 2005). In addition, it is well known that all recycled plastic, which can be melted and processed below the degradation temperature of wood or other lignocellulosic fillers, is usually suitable for manufacturing WPCs (Najafi et al. 2007). Thus, in the past decade, the utilization of recycled thermoplastics has also been considered for manufacturing WPCs (Chen et al. 2006; Adhikary et al. 2008). However, there are only a few studies concerning the performance characteristics, particularly material dispersion and density profiles, of various WPCs. It is also difficult to distinguish different types of WPCs owing to their similar appearance, resulting in difficulties in classifying and recycling, when the composites are disposed of at the end of their service life.

Fourier transform infrared (FTIR) spectroscopy is one of the most widely utilized techniques for determining molecular structures in biological samples, and it has successfully been applied for rapid detecting and identifying tree species and microbial strains (Owen and Thomas 1989; Sandt et al. 2003; Al-Qadiri et al. 2006). FTIR or Fourier transform near-infrared (FTNIR) spectroscopy combined with multivariate statistical methods can discriminate wood species, and even wood of trees from different growth habitats (Gierlinger et al. 2004; Rana et al. 2008).

The focus of the present study was on the plastic moiety of WPCs. The aims were: (1) a comparison of physicomechanical properties among different types of WPCs, (2) recording the distribution profile of wood and plastic materials in different WPCs by FTIR analysis, and (3) rapid determination of different types of WPCs by FTIR spectroscopy combined with principal component analysis (PCA).

Materials and methods

Preparation of wood particles

Trema orientalis (L.) Blume, a fast-growing wood species, was sampled from the experimental forest of National Chung Hsing University in Nan-Tou County. Wood particles were prepared by hammer-milling and sieving; particles between 6 and 16 mesh were investigated.

Plastics

Commercial virgin plastics: (1) virgin HDPE [Unithene® LH901; melt flow index (MFI): 0.95 g/10 min; density: 0.95 g cm^{-3}]; (2) LDPE (Paxothene® NA248; MFI: 46.00 g/10 min; density: 0.92 g cm^{-3}); (3) PP (Globalene® PT100; MFI: 1.60 g/10 min; density: 0.90 g cm^{-3}); (4) PS (Polyrex® PG-80; MFI: 4.00 g/10 min; density: 1.05 g cm^{-3}). Source: these materials were purchased from USI Co. (Kaohsing, Taiwan), LCY Chemical Industry Co. (Kaohsing, Taiwan), and Chi-Mei Co. (Tainan, Taiwan). A recycled HDPE (rHDPE; MFI: 0.22 g/10 min; density: 0.95 g cm^{-3}) was kindly

supplied by Orbit Polymers Co., Ltd (Taichung, Taiwan). All plastic pellets were ground in an attrition mill to reduce their particle size to less than 20 mesh before composite processing.

Composite processing

Manufacturing WPCs: the flat-platen pressing process was applied according to Chen et al. (2006). The weight ratio of oven-dried wood particles (moisture content $<3\%$) and plastic powder was 60/40 (wt%). The expected density of WPCs was 0.85 ± 0.05 g cm^{-3}. Format of the WPCs: 300 mm$\times$200 mm with 12 mm thickness. All WPCs were produced in a two-step pressing process: (1) hot pressing at 170–200°C (170°C for LDPE; 180°C for HDPE, rHDPE and PS; 200°C for PP) for 8 min; and (2) finishing by cold pressing until the temperature of the WPCs decreased to 25°C (approx. 10–12 min).

Determining the composite properties

Density, water absorption, thickness swelling, flexural properties (MOR and MOE), and internal bond strength, were determined according to the Chinese National Standard CNS 2215. Data of MOR and MOE have been obtained by the three-point static bending test with a loading speed of 10 mm min^{-1} and span of 180 mm (specimen size: $230\times50\times12$ mm^3). Internal bond strength was tested on specimens with dimensions of $50\times50\times12$ mm^3 at a tensile speed of 2 mm min^{-1}. The samples were conditioned at 20°C and 65% relative humidity for 2 weeks before testing. At least five specimens of each blend were tested.

Evaluation of the vertical density profile

The vertical density profiles of specimens (50 mm$\times$25 mm and 12 mm thickness) were analyzed using a QTRS-01X X-ray density profiler (Quintek Measurement Systems, NT, USA). Eighteen specimens of each blend were tested; measurements were taken at 0.04-mm intervals.

ATR-FTIR spectral measurements

Instrumentation for attenuated total reflection FTIR (ATR-FTIR) composites: Spectrum 100 FTIR spectrometer (Perkin–Elmer, Bucks, UK) equipped with a DTGS detector and a MIRacle ATR accessory (Pike Technologies, WI, USA). The spectra were collected by co-adding 32 scans at a resolution of 4 cm^{-1} in the range from 650 to 4000 cm^{-1}. Five spectra were acquired at room temperature for each sample to yield 25 spectra for each composite.

ATR spectra were statistically analyzed by PCA using MVSP version 3.1 software (Kovach Computing Services, Wales, UK). PCA provided graphical representations of the similarities and differences in spectral data between treatments by removing random variation and generating natural clustering within a data set (Al-Qadiri et al. 2008). PCA identifies directions (principal components, PCs) along which the variance of the data is maximal (Mansfield et al. 1997). The effect of this process is a concentration of the sources of variability of the data set into a few PCs. Plots of the PC scores (projection on to PC axes) against one another can reveal clustering or structure in the data set (Chen et al. 1998). For data analysis, the region of 1650–650 cm^{-1} of the ATR spectra was vector normalized, the second derivation was calculated, the data were used for PCA and the factor loadings were plotted.

Scanning electron microscopy

The morphology of wood particles and plastics in composites were examined by scanning electron microscopy (SEM). Following an internal bond test, the fracture surface of composites was dried and then imaged using a Hitachi TM-1000 (Japan) SEM instrument with an accelerating voltage of 15 kV. The samples were viewed perpendicular to the fractured surface.

Analysis of variance

All results were expressed as mean$\pm$SD. The significance of difference was calculated by Scheffe's test; P values <0.05 were considered to be significant.

Results and discussion

Physicomechanical properties of different types of WPCs

Some physicomechanical properties of the composites are listed in Table 1. The density of all samples ranged from 0.81 to 0.84 g cm^{-3} and there were no significant differences among them. However, after 24 h of water immersion, the thickness swelling and water absorption of immersed samples were significantly influenced by the type of plastic in the WPCs. The composites made from PS have the highest thickness swelling (6.8%) and water absorption (31.1%). By contrast, the HDPE- and rHDPE-based composites show the lowest values without significant differences between these two composites. It is well known that the moisture absorption in composites is mainly owing to the gaps and flaws at the interfaces, and the microcracks in the matrix formed during the process (Adhikary et al. 2008) in addition to the hydrophilic nature of wood flour. The amount of wood particle

Table 1 Influence of plastic types on the physicomechanical properties of WPCs.

WPC	Density (g cm^{-3})	Effects of 24 h soaking		MOR (MPa)	MOE (GPa)	Internal bond (MPa)
		Thickness swelling (%)	Water absorption (%)			
HDPE	0.84 ± 0.02^{a}	4.0 ± 0.4^{c}	11.8 ± 1.3^{b}	21.0 ± 1.9^{b}	1.7 ± 0.1^{a}	2.2 ± 0.2^{a}
rHDPE	0.83 ± 0.02^{a}	4.3 ± 0.2^{c}	12.7 ± 2.5^{b}	20.3 ± 0.9^{b}	1.7 ± 0.2^{a}	2.2 ± 0.2^{a}
LDPE	0.81 ± 0.01^{a}	5.7 ± 0.2^{ab}	13.3 ± 0.7^{b}	8.5 ± 0.7^{c}	1.1 ± 0.1^{b}	0.7 ± 0.1^{c}
PP	0.82 ± 0.02^{a}	4.8 ± 1.1^{bc}	21.5 ± 6.6^{ab}	25.3 ± 1.4^{a}	2.0 ± 0.2^{a}	2.2 ± 0.2^{a}
PS	0.81 ± 0.02^{a}	6.8 ± 0.9^{a}	31.1 ± 7.3^{a}	20.0 ± 3.2^{b}	2.0 ± 0.2^{a}	1.4 ± 0.4^{b}

Values are mean$\pm$SD (n=5). Different letters within a column indicate significant difference at $P<0.05$.

was constant in all composite formulations. Accordingly, these results indicate that PS is the least effective plastic to form good interfaces to wood and thus leads to the highest water uptake.

Table 1 also shows that the MOR of composites ranged from 8.5 to 25.3 MPa. The highest bending strength was found in PP-based composite, followed by HDPE-, rHDPE-, PS-, and LDPE-based composites. In general, it is well known the mechanical behavior of neat plastics decrease in order of PP > PS > HDPE > LDPE. Accordingly, the strength of other WPCs displayed the same trend as the neat plastics, except for the PS composite. In addition, the mechanical properties of the specimen containing recycled plastic (rHDPE) were statistically similar and comparable with those of the composite made from virgin HDPE. Similar results were reported by Najafi et al. (2006) and Adhikary et al. (2008). Obviously, recycled plastics are suited for manufacturing WPCs. Composites produced from PS showed statistically lower internal bond strength (1.4 MPa) compared with recycled (2.2 MPa) and virgin HDPE composites (2.2 MPa). This can be mainly attributed to poor interfacial interaction between the polymeric matrix and wood particle, not allowing efficient stress transfer between the two phases of the material (Shibata et al. 2002). Figure 1 provides the SEM micrographs of the fracture surfaces of the five composites. It is a remarkable difference in the wood particle-matrix interaction between the PS and the other four composites. No matrix residue is left on the surface of wood particles from the PS composite, in contrast to the surface of other composites, which are covered by layers of matrix material being pulled out together with particles. Again, it can be safely concluded that in PS composites failures occur at the wood particle-matrix interface as a result of a less effective wood particle wetting by the polymeric matrix.

Distribution profile of wood and plastic materials in various WPCs

It is well known that the uniformity of lignocellulosic materials dispersed in a polymeric matrix greatly affects the mechanical behavior of composites (Raj et al. 1989; Chen et al. 2006). Traditionally, the fiber organization within composites is observed by SEM, but the quantitative determination of the wood-plastic profiles is difficult to realize with SEM. By contrast, ATR-FTIR spectroscopy is considered as a simple, direct, flexible, and sensitive in situ characterization technique also for wood and wood-based composites, the results of which can also be quantified (Stark and Matuana 2007; Rana et al. 2008). In this study, the ATR-FTIR spectroscopy was used to characterize the distribution profile of wood and plastic materials in the thickness direction. Figure 2 presents the spectra of the plastics and wood. Wood has a specific absorption band at 1033 cm^{-1} (cellulose C-O stretch). However, this band was not visible in the spectra of the plastics. Instead, all spectra of HDPE, rHDPE, LDPE, and PP displayed a strong absorption band at 2916 cm^{-1} (asymmetric CH_2 stretch). An exception was the spectrum of the PS, which showed a specific band at 696 cm^{-1} (=C-H out-of-plane deformation). ''Plastic indices'' (PI) were calculated based on the absorbance ratios of 696 cm^{-1}/1033 cm^{-1} for PS composite and 2919 cm^{-1}/1033 cm^{-1} for the other four composites.

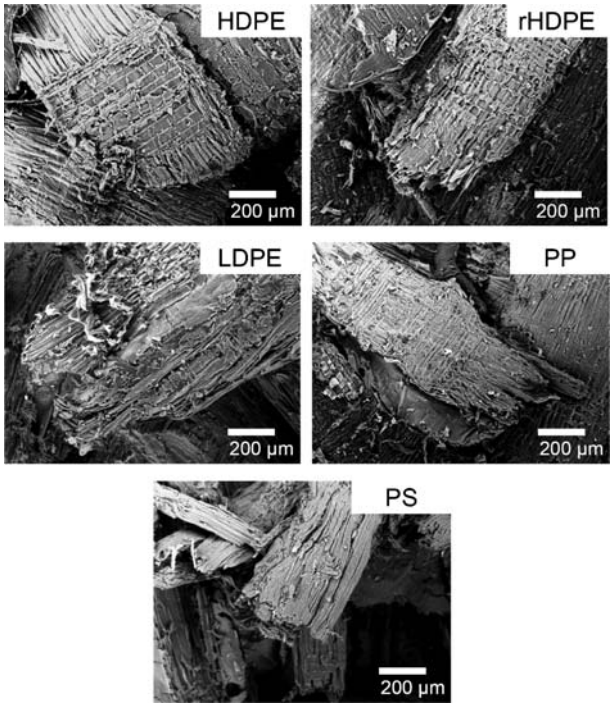

Figure 1 SEM micrographs of different WPCs.

The regression equations related the PI to a measurable plastic content in each WPC are presented in Table 2. It is remarkable that all R^2 values are higher than 0.99. Based on these equations, the distribution profile of plastic in the thickness direction is shown in Figure 3. As observed, the plastic contents of the surface layer of HDPE, rHDPE, and PP composites were significantly higher than the core layer, whereas homogenous dispersion was noted in the LDPE composite. Among all WPCs, however, the PS composite displayed the worst dispersion. Therefore, wood particles did not have a uniform distribution in this composite, which can also be interpreted as a poor particle encapsulation by the polymer.

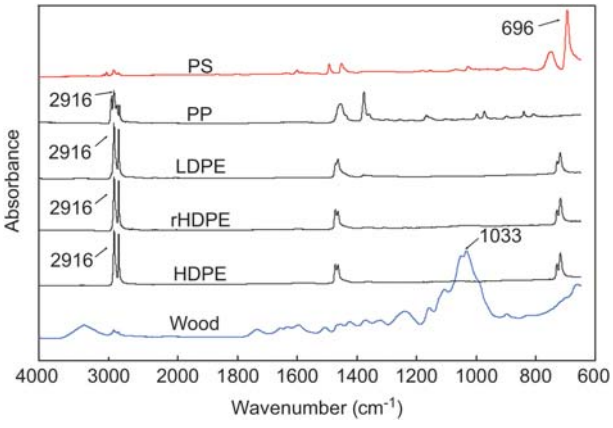

Figure 2 ATR-FTIR spectra of wood and plastics.

Table 2 Regression equations for the plastic content of various WPCs.

Polymer	Regression equation[a]	R^2
HDPE	Plastic cont.=35.230 PI+16.279	0.992
rHDPE	Plastic cont.=45.399 PI+9.514	0.998
LDPE	Plastic cont.=35.753 PI+17.029	0.994
PP	Plastic cont.=107.120 PI-1.088	0.992
PS	Plastic cont.=44.315 PI-3.937	0.990

[a]Weight ratios of wood particle to plastic ranged from 20 to 80 wt%.
PI, plastic indices calculated based on FTIR spectra.

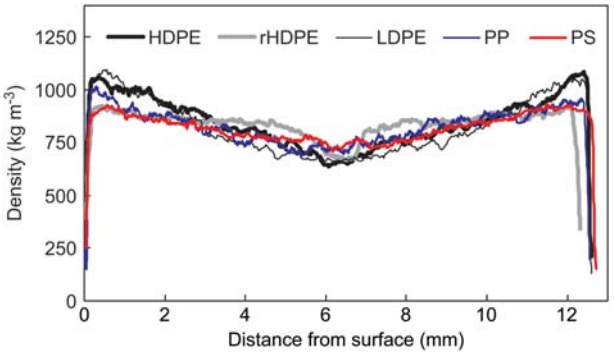

Figure 4 Vertical density profiles of WPCs produced from different plastics.

This is in agreement with the higher water absorption and thickness swelling of the PS-wood composite.

By contrast, as shown in Figure 4, the vertical density profile of all composites resembles a flat 'V-shape', which is similar to the typical vertical density profile of the particleboards produced by conventional hot pressing (Wong et al. 1999).

Distinguishing WPCs by ATR-FTIR spectroscopy combined with PCA

It is difficult to identify a WPC-type by its physicomechanical properties. However, vibrational spectroscopy could be a suitable method for this purpose (Faix 1991; Kotilainen et al. 2000). Thus in this study, ATR-FTIR spectroscopy was combined with PCA to discriminate WPC species. It is well known that spectra converted into their second derivative has several advantages: the influence of base-line shift is diminished and thus the reproducibility of spectra is elevated (Kansiz et al. 1999); moreover, typical spectral features are easier to discriminate (Sandt et al. 2003). A mean-centered PCA was conducted based on the second derivative ATR spectra over the range of 1650–650 cm^{-1} (Figure 5a). Distinct segregation and clustering between the five WPCs are apparent. In the score plot, a robust separation between WPCs was easily achieved by combining principal component 1 (PC1) with principal component 2 (PC2). As is visible, WPCs produced from polyethylene (HDPE, rHDPE, and LDPE) were well separated from other composites, and the LDPE- and HDPE-based composites could also be discriminated. Similarly, WPCs produced from PS or PP are also clearly differentiated from all other WPCs. These differentiations most probably reflect formulation and matrix differ-

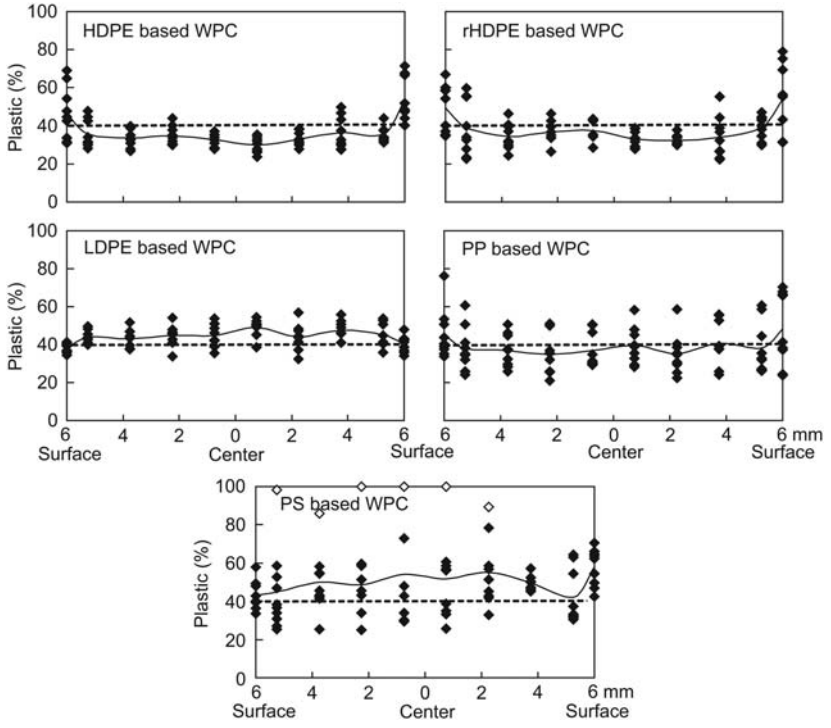

Figure 3 The distribution profile of wood and plastic materials in the thickness direction for different WPCs. ♦: data were obtained by interpolation; ◇: data were obtained by extrapolation.

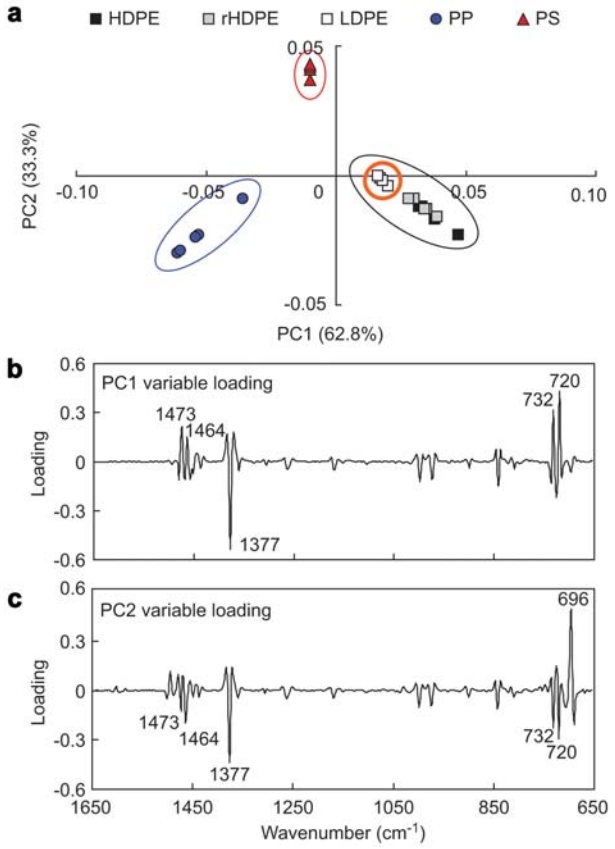

Figure 5 Principal component analysis (PCA) of second-derivative ATR-FTIR spectral regions (1650–650 cm^{-1}) for different WPCs: (a) score scatter plot of PC1 versus PC2; (b) PC1 loading profile; (c) PC2 loading profile.

ences in various WPCs. Not unexpectedly, only the differentiation between the virgin and recycled HDPE composites was difficult because of the same chemical nature of these plastics.

Loading plots were generated to highlight the contribution of each variable (wavenumber) to each principal component (Kansiz et al. 1999). The first and second principal components from PCA in the range of 1650–650 cm^{-1} are shown in Figure 5b,c. Large positive or negative loadings are generally associated with spectral regions responsible for polymeric matrix differentiation. Over the range of 1650–650 cm^{-1}, PC1 and PC2 accounted for 96.1% of the total variability (62.8 and 33.3%, respectively). Through inspection of the PC1 loading profile (Figure 5b), it is clear that the major contributions to spectral variation are the methylene scissoring (δ_s CH_2) and rocking (ρ CH_2) vibrations at 1473, 1464, 732, and 720 cm^{-1}. Of these, the doublet peaks observed at 1473–1464 and 732–720 cm^{-1} correspond to the crystalline (1473 and 732 cm^{-1}) and amorphous content (1464 and 720 cm^{-1}) of polyethylene (Stark and Matuana 2004). Additionally, a major negative band at 1377 cm^{-1} is attributed to the symmetric methyl bending vibration of PP (branched-chain) (Arkatkar et al. 2009). By contrast, the WPCs produced from PS are clearly distinguished from all remaining ones, being located on the positive PC2 axis (Figure 5a). The corresponding PC2 loading (Figure 5c) clearly shows the origin of the observed sample separation: it is a significant absorption peak appearing at 696 cm^{-1}. This characteristic peak corresponds to the CH out-of-plane deformation in the benzene ring of the PS-based composites (Matusinović et al. 2008).

Conclusions

The physicomechanical properties of WPCs are greatly influenced by the dispersion of lignocellulosic materials and the type of plastic present in WPCs. Composites containing HDPE (virgin and recycled) displayed the best dimension stability and water absorption resistance, whereas the PS-based composite displayed the worst. As for mechanical properties, the PP-based composite showed the strongest bending strength, followed by HDPE, rHDPE, PS, and LDPE composites. ATR-FTIR spectroscopy has successfully been applied for determining the distribution profile of wood and plastic materials within WPCs. Furthermore, ATR-FTIR combined with PCA succeeded to discriminate WPC species. Different types of WPCs can be clearly distinguished by this method; in particular, it is well suited for differentiating between LDPE and HDPE composites. In future investigations, the weatherability and durability of different types of WPCs will be monitored by ATR-FTIR/PCA to understand the major chemical differences during different exposure times.

Acknowledgements

We thank the National Science Council for financial support (NSC97-2313-B-005-044-MY3).

References

Adhikary, K.B., Pang, S., Staiger, M.P. (2008) Dimensional stability and mechanical behaviour of wood-plastic composites based on recycled and virgin high-density polyethylene (HDPE). Composites B 39:807–815.

Al-Qadiri, H.M., Lin, M., Cavinato, A.G., Rasco, B.A. (2006) Fourier transform infrared spectroscopy, detection and identification of *Escherichia coli* O157:H7 and *Alicyclobacillus* strains in apple juice. Int. J. Food Microbiol. 111:73–80.

Al-Qadiri, H.M., Al-Alami, N.I., Al-Holy, M.A., Rasco, B.A. (2008) Using Fourier transform infrared (FT-IR) absorbance spectroscopy and multivariate analysis to study the effect of chlorine-induced bacterial injury in water. J. Agric. Food. Chem. 56: 8992–8997.

Arkatkar, A., Arutchelvi, J., Bhaduri, S., Uppara, P.V., Doble, M. (2009) Degradation of unpretreated and thermally pretreated polypropylene by soil consortia. Int. Biodeterior. Biodegrad. 63: 106–111.

Ashori, A. (2008) Wood-plastic composites as promising green-composites for automotive industries! Bioresour. Technol. 99: 4661–4667.

Bengtsson, M., Gatenholm, P., Oksman, K. (2005) The effect of crosslinking on the properties of polyethylene/wood flour composites. Comp. Sci. Technol. 65:1468–1479.

Chen, H.C., Chen, T.Y., Hsu, C.H. (2006) Effects of wood particle size and mixing ratios of HDPE on the properties of the composites. Holz Roh- Werkst. 64:172–177.

Chen, L., Carpita, N.C., Reiter, W.D., Wilson, R.H., Jeffries, C., McCann, M.C. (1998) A rapid method to screen for cell-wall mutants using discriminant analysis of Fourier transform infrared spectra. Plant J. 16:385–392.

Faix, O. (1991) Classification of lignins from different botanical origins by FTIR spectroscopy. Holzforschung 45:21–27.

Gierlinger, N., Schwanninger, M., Wimmer, R. (2004) Characteristics and classification of Fourier-transform near infrared spectra of heartwood of different larch species (*Larix* sp.). J. Near Infrared Spectr. 12:113–119.

Harper, D., Wolcott, M. (2004) Interaction between coupling agent and lubricants in wood-polypropylene composites. Composites A 35:385–394.

Kansiz, M., Heraud, P., Wood, B., Burden, F., Beardall, J., McNaughton, D. (1999) Fourier transform infrared microspectroscopy and chemometrics as a tool for the discrimination of cyanobacterial strains. Phytochemistry 52:407–417.

Klyosov, A.A. Wood-Plastic Composites. John Wiley & Sons, New Jersey, 2007.

Kotilainen, R.A., Toivanen, T.J., Alén, R.J. (2000) FTIR monitoring of chemical changes in softwood during heating. J. Wood Chem. Technol. 20:307–320.

Lei, Y., Wu, Q. (2010) Wood plastic composites based on microfibrillar blends of high density polyethylene/poly(ethylene terephthalate). Bioresour. Technol. 101:3665–3671.

Mansfield, J.R., Sowa, M.G., Scarth, G.B., Somorjai, R.L., Mantsch, H.H. (1997) Fuzzy C-means clustering and principal component analysis of time series from near-infrared imaging of forearm ischemia. Comp. Med. Imag. Graph. 21:299–308.

Matusinović, Z., Rogošić, M., Šipušić, J., Macan, J. (2008) Polymer nanocomposite materials based on polystyrene and a layered aluminate filler. Polym. Eng. Sci. 48:2027–2032.

Nair, K.C.M., Thomas, S., Groeninckx, G. (2001) Thermal and dynamic mechanical analysis of polystyrene composites reinforced with short sisal fibres. Comp. Sci. Technol. 61:2519–2529.

Najafi, S.K., Hamidinia, E., Tajvidi, M. (2006) Mechanical properties of composites from sawdust and recycled plastics. J. Appl. Polym. Sci. 100:3641–3645.

Najafi, S.K., Tajvidi, M., Hamidina, E. (2007) Effect of temperature, plastic type and virginity on the water uptake of sawdust/plastic composites. Holz Roh- Werkst. 65:377–382.

Owen, N.L., Thomas, D.W. (1989) Infrared studies of ''Hard'' and ''Soft'' woods. Appl. Spectr. 43:451–455.

Raj, R.G., Kokta, B.V., Maldas, D., Daneault, C. (1989) Use of wood fibers in thermoplastics. VII. The effect of coupling agents in polyethylene-wood fiber composites. J. Appl. Polym. Sci. 37:1089–1103.

Rana, R., Műller, G., Naumann, A., Polle, A. (2008) FTIR spectroscopy in combination with principal component analysis or cluster analysis as a tool to distinguish beech (*Fagus sylvatica* L.) trees grown at different sites. Holzforschung 62:530–538.

Rothlin, O. (2007) Processing wood–plastic composites places new demands on feeders. Plast. Addit. Comp. 9:36–39.

Sandt, C., Sockalingum, G.D., Aubert, D., Lepan, H., Lepouse, C., Jaussaud, M., Leon, A., Pinon, J.M., Manfait, M., Toubas, D. (2003) Use of Fourier-transform infrared spectroscopy for typing of *Candida albicans* strains isolated in intensive care units. J. Clin. Microbiol. 41:954–959.

Shibata, M., Takachiyo, K., Ozawa, K., Yosomiya, R., Takeishi, H. (2002) Biodegradable polyester composites reinforced with short abaca fiber. J. Appl. Polym. Sci. 85:129–138.

Stark, N.M., Matuana, L.M. (2004) Surface chemistry and mechanical property changes of wood-flour/high-density-polyethylene composites after accelerated weathering. J. Appl. Polym. Sci. 94:2263–2273.

Stark, N.M., Matuana, L.M. (2007) Characterization of weathered wood–plastic composite surfaces using FTIR spectroscopy, contact angle, and XPS. Polym. Degrad. Stab. 92:1883–1890.

Wong, E.D., Zhang, M., Wang, Q., Kawai, S. (1999) Formation of the density profile and its effects on the properties of particleboard. Wood Sci. Technol. 33:327–340.

Received December 15, 2009. Accepted May 10, 2010.
Previously published online July 29, 2010.